Indian Journal of Pure & Applied Physics
Vol. 62, January 2024, pp. 29-37
DOI: 10.56042/ijpap.v62i1.4078

Tropical Ionospheric response to Very Severe Cyclonic Storm "BULBUL" observed over SANYA (18.34°N, 109.62°E)

G J Bhagavathiammal[a,b*] & M Gajalakshmi[a]

[a]Department of Medical Physics, Sir C V Raman Science Block, Anna University, Sardar Patel Road, Guindy, Chennai 600 025, India
[b]Centre for Climate Change & Disaster Management (CCCDM), Anna University, Sardar Patel Road, Guindy, Chennai 600 025, India

Received 17 July 2023; accepted 28 November 2023

We present the tropical ionospheric response to a severe cyclonic storm, "BULBUL," observed from Ionosonde observations over "SANYA" (18.34°N, 109.62°E). The cyclone "BULBUL" developed as a low pressure on 5 November 2019 and intensified into a Very Severe Cyclonic Storm (VSCS) on 8 November 2019, and a landfall occurred on 9 November 2019 over West Bengal. This study utilizes Ionospheric parameters foF2 and hmF2 during the cyclone (5-11 November 2019). The cyclone period falls under quiet geomagnetic conditions (Kp < 3) and makes us investigate the lower atmospheric meteorological event's impacts on the ionosphere. Significant modulation has been found in hmF2 and foF2 during cyclone-intensified stages (SCS, VSCS, Land fall) from 7-9 November 2019. Low OLR and upward vertical velocity are observed at the matured stages, suggesting deep convection, generating Gravity Wave Oscillations. Local time profile reveals the severe suppression in foF2 during the intensification and land falling day of the cyclone, and reversely hmF2 shows an increasing trend. The peak value of hmF2 shifted from post-noon to prenoon hours during the progression of the cyclone (from SCS to VSCS and landfall). In addition, we observed strong gravity wave oscillations of about ~3 and 5 hours in foF2.

Keywords: Ionosphere; Tropical Cyclone; BULBUL; foF2; hmF2; Gravity Waves

1 Introduction

Tropical cyclones are devastating natural hazardous tropical weather systems that cause severe damage/threat to society, economic loss, and human casualties due to strong winds, heavy rainfall, flooding, and storm surges[1-4]. Recent studies suggested significant changes in land, ocean, and atmospheric parameters during tropical cyclones. Recently, Perez-Alarcon *et al.*[5] reported that tropical cyclones have been intensified by 17% and increased the frequency of cyclone occurrence due to increased anthropogenic climate activities. Five decades of atmospheric research reported the significant influence of tropical cyclones on ionospheric dynamics. However, the mechanism is still puzzling, and more investigation is needed to understand the tropical cyclone–ionosphere coupling.

Numerous authors have extensively studied the linkage between tropical cyclones and the ionosphere using state-of-the-art observations like GPS, GNSS, VLF, and Ionosonde observations. These studies summarize the outcome as a significant variation in Total Election Content[6-12], Travelling Ionospheric Disturbances (TIDs) in the Ionosphere[13-15], VLF signal anomalies[16-20], variation in Ionospheric parameters like foF2 and hmF2[21-24] and maximum distortion in radio wave communication[25].

The two-way critical relationship of tropical cyclone–ionosphere coupling was reported by Vanina et al. [26]. One way is through dynamical coupling - generation and propagation of tropical storm-induced atmospheric waves such as gravity, tidal, and planetary waves [27,28] and electrical coupling. Gravity waves are buoyancy oscillations of periods from minutes to several hours, originating from tropical cyclone-induced convection. Several studies reported these gravity waves introduce significant changes in the Ionosphere[6,9,18,21-22,29-34].

Tropical cyclone "BULBUL" is a Very Severe Cyclonic Storm (VSCS) formed over the Bay of Bengal that caused heavy rainfall, flood, and storm surges. Faisal *et al.*[35] simulated the storm surge height during BULBUL using the Meteorological Research Institute (MRI) model. Kumar *et al.*[36] predicted the cyclone intensity, location, and time of landfall for cyclone "BULBUL". Biswakarma *et al.*[37] studied the water inundation assessment during the "BULBUL" cyclone using remote sensing and Geographic Information System (GIS) tools.

*Corresponding author: (E-mail: selvigjb@gmail.com)

The present work investigates the ionospheric response to the Very Severe Cyclonic Storm "BULBUL" (5-11 November 2019) observed over the tropical site "SANYA "(18.34°N, 109.62°E, dip angle 27.12°). SANYA site is situated in the low latitude band with geographic coordinates latitude 18.34°N and longitude 109.62°E, and its geographic location is shown in Fig. 1. The ionospheric parameters foF2 and hmF2 were utilized in this study to investigate the tropical cyclone effects on the ionosphere. The Ionospheric foF2 and hmF2 were retrieved by a real-time ionogram scaler with true-height analysis[38]. The cyclone "BULBUL" developed as a low pressure on 5 November 2019 and intensified into a Very Severe Cyclonic Storm (VSCS) on 8 November 2019, and landfall occurred on 9 November 2019 over West Bengal.

2 Data Used & Methodology

2.1 Surface parameters from India Meteorological Department

The present study utilized surface variables like central pressure, maximum sustained wind speed, and cyclone track from the India Meteorological Department (IMD), New Delhi https://rsmcnew delhi.imd.gov.in/index.php. The maximum sustained surface wind represents the estimated highest 3-min surface wind measured at the 10m height level.

2.2 3-Hr Kp index

The Kp index indicates disturbances in the Earth's magnetic field. The mean standardized Kp-index was derived from coordinated multiple magnetic observations covering latitude 44-60° of northern or southern latitudes. The Ionosphere is a dynamically active medium that is always influenced by forcing from above (mainly geomagnetic storms) and forcing from below (meteorological events and lower atmospheric forcing). The Kp-index depicts the condition of solar and geomagnetic activities, which controls primarily ionospheric behaviour. Its value ranges from a scale of 0 to 9. The 3-Hr Kp index value below 3 is considered a geomagnetically quiet condition[39]. The cyclone "BULBUL" falls under geomagnetic quiet conditions. Hence, the impact of upper atmospheric forcing is negligible. The 3-Hr Kp index was retrieved from the World Data Centre of Geomagnetism, Kyoto http://wdc.kugi.kyoto-u.ac.jp/wdc/Sec3.html

2.3 Ionospheric Sounding over SANYA (18.34°N, 109.62°E)

Ionosonde is a radar instrument used to examine the Ionospheric behaviour. Ionosonde transmits RF power pulses vertically upward and receives reflected signals, and the response would be seen in an Ionogram profile, an altitude plot against frequency. SANYA, China, is located in a low latitude belt with geographic coordinates latitude 18.34°N and longitude 109.62°E, and the geographic location is shown in Fig. 1. The ionospheric parameters, namely, foF2 (Critical frequency of F2 layer) and hmF2 (peak height of F2 layer), were retrieved with the help of an automatic real-time ionogram scaler with true height analysis[38]. The scaled hourly Ionospheric foF2 and hmF2 for the station “SANYA” were obtained from the World Data Centre (WDC) for Geophysics, Beijing, supported by

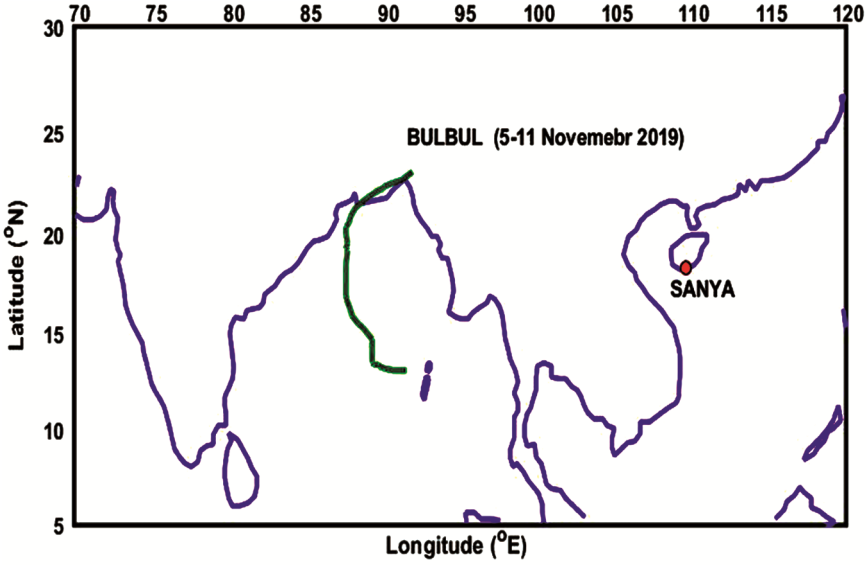

Fig. 1 — Map representation of Cyclone BULBUL (green line) and the observatory site SANYA (18.34°N, 109.62°E).

the Institute of Geology and Geophysics, Chinese Academy of Sciences (IGGCAS), an international research centre well equipped with strong basic research and resources for technological innovation on the frontiers of the solid Earth and Space Sciences.

2.4 ECMWF ERA5 Reanalysis

The lower atmospheric dynamical variables were achieved from ERA 5 Reanalysis datasets. ERA 5 is the fifth generation European Centre for Medium-Range Weather Forecasts (ECMWF) atmospheric reanalysis of the global climate covering from 1940 to the present. The dynamical variable vertical velocity is utilized from ERA 5 Reanalysis[40], operated by Copernicus Climate Change Service. The vertical velocity is obtained from CDS Cloud Server https://cds.climate.copernicus.eu/.

2.5 Outgoing Longwave Radiation

The daily interpolated Outgoing Longwave Radiation (OLR) data was obtained from the Climate Diagnostic Center (CDC), National Oceanic and Atmospheric Administration (NOAA) with the spatial resolution of 1° latitude × 1° longitude grid.

2.6 Cyclone "BULBUL"

The Very Severe Cyclonic Storm "BULBUL"[41] over the northwest Bay of Bengal moved nearly northward with a speed of 12 kmph and lay centred on 9 November 2019 over the northwest Bay of Bengal near Latitude 20.65°N and Long 87.85°E about 125m east-northeast of Odisha. It weakened gradually, moved north-eastwards, and crossed the West Bengal - Bangladesh Coasts between Sagar Islands (West Bengal) and Khepupara (Bangladesh) across the Sunderban delta by late evening/ night (between 20:00 & and 23:00 hours IST) of 9 November as a Severe Cyclonic Storm with a maximum sustained wind speed of 110-120 Kmph gusting to 135 Kmph.

Figure 1 shows the geographic map representation of cyclone track "BULBUL" during 5-11 November 2019. The cyclone track is plotted in a green line, and the observation site "SANYA (18.34°N, 109.62°E) is marked in a red circle. The distance between the cyclone position and SANYA is ~20°. Table 1 shows the intensification stages of cyclone "BULBUL" and its distance from the observation site "SANYA".

3 Results and Discussion

3.1 Surface Variabilities during BULBUL

Figure 2 represents the temporal variation of surface variables, such as sustained wind speed and estimated central pressure during cyclone "BULBUL". The

Table 1 — Progress of Cyclone BULBUL

Date/UT	Position		Maximum sustained surface wind speed (kt)	Stages of cyclone	Distance: Cyclone position from SANYA(Degree)
	Lat. (^{0}N)	Long. (^{0}E)			
05.11.19/0300	13.1	91.0	20 gusting to 25	Depression	18.21°
06.11.19/0000	13.4	89.7	25 gusting to 30	Deep Depression	19.79°
07.11.19/2100	16.6	87.7	30 gusting to 60	Severe Cyclonic Storm	20.9°
08.11.19/1200	18.5	87.6	maximum of 75	Very Severe Cyclonic Storm	20.9°
09.11.19/1500	21.4	88.3	Reduced to 60	Severe Cyclonic Storm	20.3°
10.11.19/0900	22.4	90.1	Reduced to 30	Deep Depression	18.7°
11.11.19/0000	23.1	91.9	Reduced to 20	Depression	17.3°

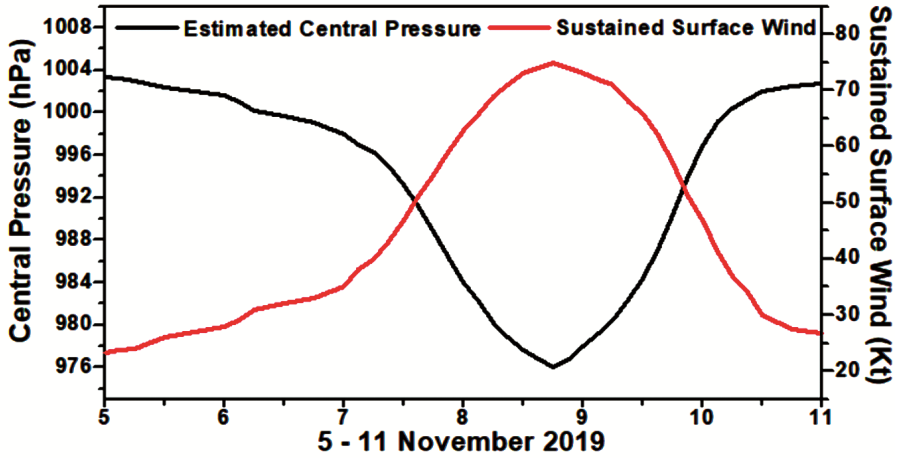

Fig. 2 — Temporal variation of Central Pressure (black line) and Maximum Sustained Surface wind (red line) during cyclone BULBUL

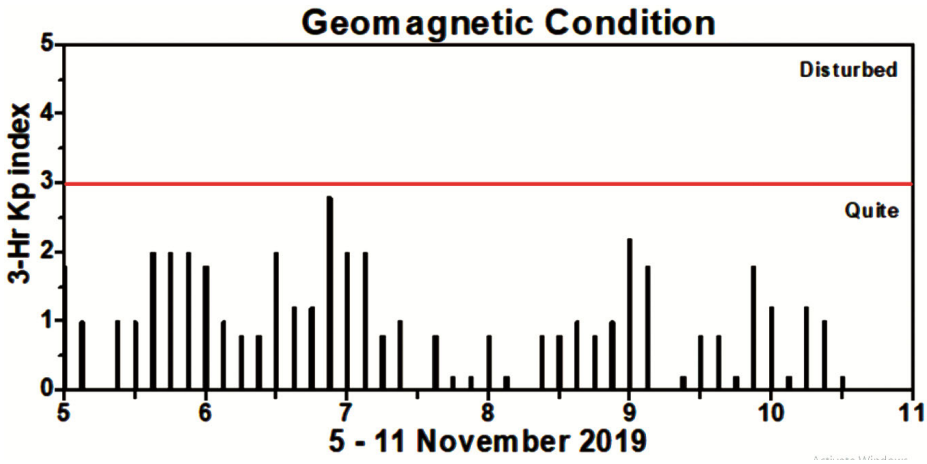

Fig. 3 — Geomagnetic condition during cyclone BULBUL.

cyclone progressed from Depression on 05 November 2019. It further intensified and became a Very Severe Cyclonic Storm on 08 November 2019. As the cyclone intensifies, the central pressure decreases, and reversely sustained wind speed decreases steadily. The central pressure reached its minimum (976hPa), and sustained wind speed reached its maximum (~75 kt) on 8 November 2019. The trend reversed during cyclone decay on 10 and 11 November 2019. It clearly shows the negative correlation between sustained wind speed and central pressure. Cyclonic wind speed is measured by the pressure gradient or the lowest pressure difference between the storm centre and the storm's outside pressure, divided by the distance in which the pressure change occurs.

3.2 Ionospheric variation during "BULBUL" cyclone

Figure 3 shows the geomagnetic condition during cyclone "BULBUL". The 3-Hr Kp index less than (Kp < 3) during the cyclonic period 5-11 November 2019 indicates the quiet geomagnetic condition.

Figure 4(a) shows the temporal variation of foF2 (top) and hmF2 (bottom) during cyclone BULBUL. To visualize the tropical cyclone effect on foF2 and hmF2, we have taken a mean 10-quiet-day variation of foF2 and hmF2 as a reference, and a black line denotes it. The peak foF2 decreased on 06 November 2019 after the Deep Depression of cyclone BULBUL. At intensified stages (07-09 November 2019), a significant reduction in foF2 is found from the reference. The peak foF2 shows a substantial decrease of about ~1 MHz, ~0.8 MHz and ~2 MHz on 7-9 November 2019 from the reference. Whether as, peak hmF2 shows a modulating pattern during cyclone "BULBUL". The peak hmF2 increased by about 25 km and ~28 km on the 8th and 9th of November 2019 before noon hours. On the intensified stages of cyclone BULBUL (7-9 November 2019), foF2 and hmF2 show a negative correlation trend.

Figure 4(b) represents the local time variation of foF2 (left) and hmF2 (right) for 0-9 UT during the cyclone BULBUL. As we can see from Figure 4(b), the foF2 and hmF2 show maximum variation around 4-9UT. In SCS/VSCS, as we infer from the BULBUL cyclone, significant suppression of foF2 and enhancement of hmF2 were noticed at the cyclone's intensified SCS and VSCS stages. A decrease of ~1 MHz was observed on the land falling day of the cyclone. The low foF2 and high hmF2 were observed at land falling. The reverse of the same (high foF2 and low hmF2) was found at the time of weakening of the cyclonic storm into Depression. Thus, the foF2 and hmF2 show modulating patterns during the intensified cyclone stages.

Figure 5 describes the time-latitude cross-section of OLR (bottom) and vertical velocity at 200mb (top) averaged over 85-95^{o}E & 13-25^{o}N during the cyclone BULBUL. A low OLR (<160 W/m2) declined sharply, propagating from 25^{o}N to 5^{o}N as the cyclone progressed from 5 November to 11 November 2019. OLR is an indicator of cloud top heights. Low OLR informs the presence of very high and cold clouds at tropical latitudes, which are presumed to be associated with deep convection. During the OLR drop, the vertical velocity also showed a negative low during the intensified cyclonic stages from 05 to 09 November 2019. The negative vertical velocity values indicate ascending air and positive values denote

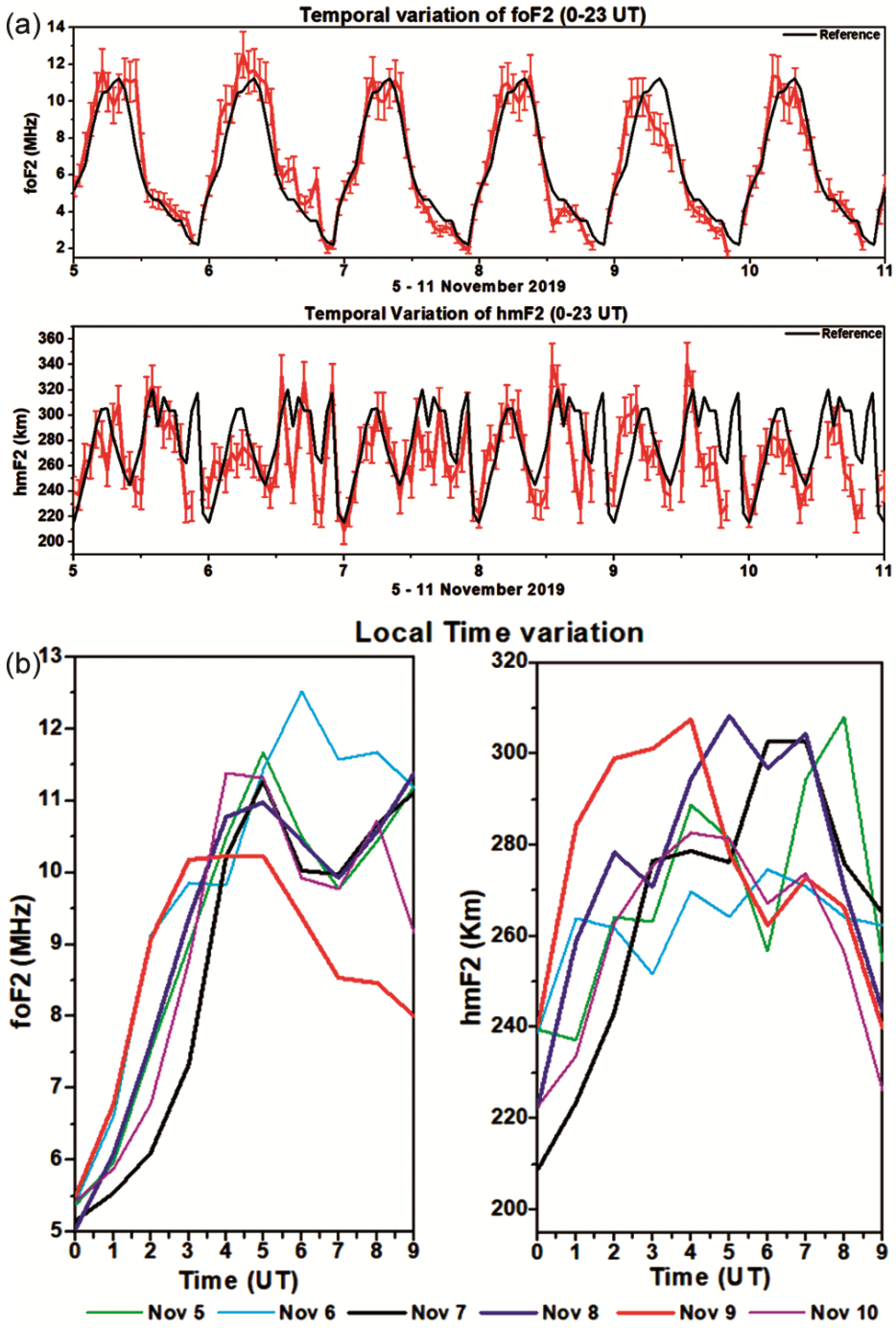

Fig. 4 — (a) Temporal variation of foF2 and hmF2 during Cyclone BULBUL. (b) Local time variation of foF2 and hmF2 during cyclone BULBUL.

sinking air. Ascending air motion is associated with cloudiness and rain. This large upward motion during the cyclonic period leads to rainfall/convection.

Figure 6 shows the mean daytime ionospheric foF2 and hmF2 variation (0-9UT) for the cyclone "BULBUL". During 7-9 November, low foF2 and high hmF2 are observed, indicating that strong anti-correlation exists between foF2 and hmF2 during the intensified cyclone stages.

Figure 7 displays the ionospheric NmF2 (top), foF2 (middle) and hmF2 (bottom) response to the cyclone "BULBUL". The top and bottom panels describe the

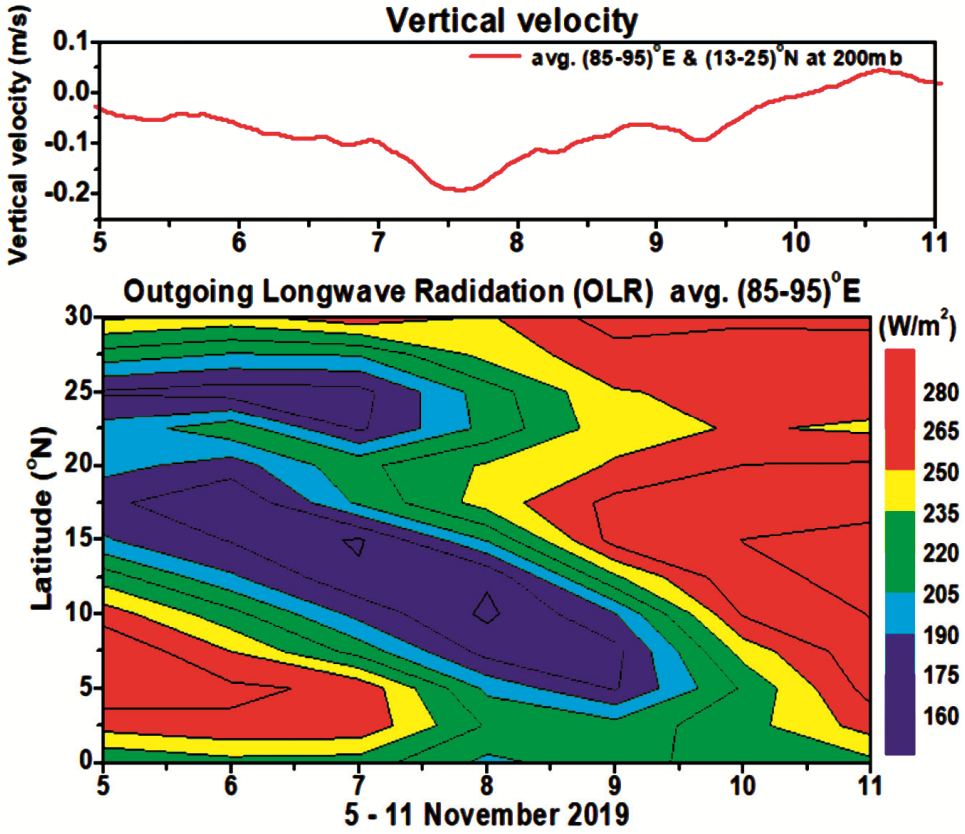

Fig. 5 — Time series of OLR and Vertical Velocity at 200mb variation averaged (85-95) °E & 13-25°N during BULBUL cyclone.

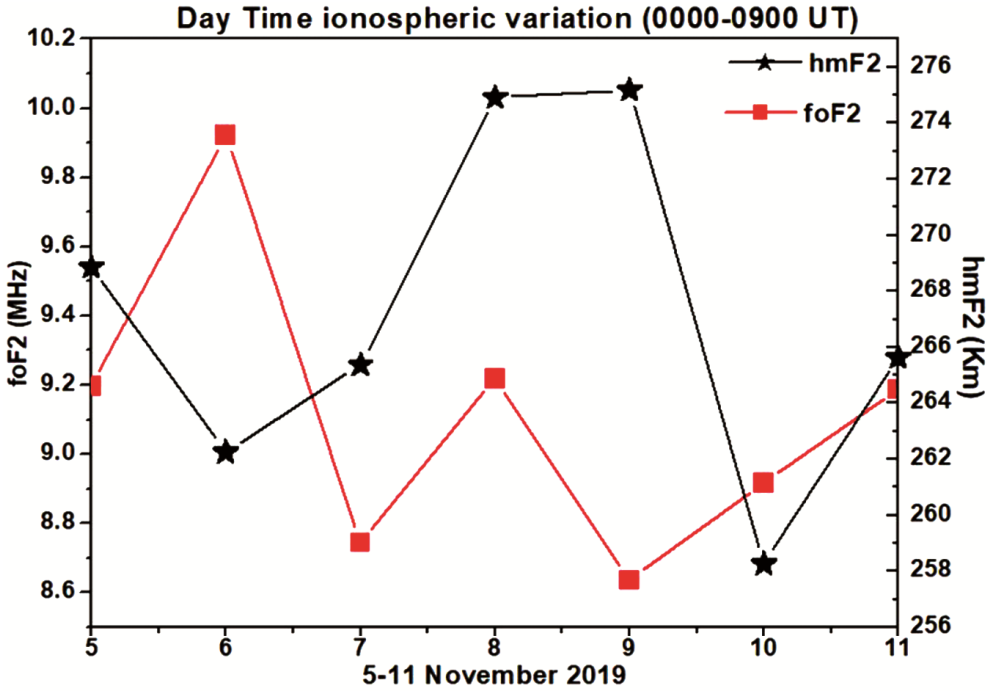

Fig. 6 — Daytime variation of foF2 and hmF2 during cyclone BULBUL.

depletion of number density and critical frequency of F2 around 4-6 UT hours during the intensified cyclone stages (7-10 November 2019). (SCS/VSCS and land fall). In reverse, the drastic enhancement in hmF2 is seen around 2-8 UT hours during the intensified cyclone stages from 7-9 November 2019. No evidence of hmF2 increase is found on 5-6 November and 10-11 November 2019.

Tropical cyclone-induced gravity waves can propagate upward to the ionosphere and interact with the background flow as Travelling Ionospheric Disturbances (TIDs). Fig. 8 depicts the wavelet spectrum of gravity wave activity in foF2 and hmF2 during the cyclone BULBUL. It describes the signatures of gravity waves with periods of ~5 hours in foF2 and hmF2. In addition, we found that a ~3-4 hr gravity wave in foF2 was observed at the start of the cyclone. The Gravity waves of period 5-hrs were observed strongly in foF2 during the intensified cyclone stages on 7-8 November 2019, but then it was observed weakly in hmF2.

Several studies reported the decrease of foF2 and TEC during tropical cyclone BULBUL as similar to cyclone events, Typhoon GILLIAN[10], TC VEENA[23], AILA AND WARD[21], TC Ockhi[22], TC AMPHAN[24]. As the tropical cyclone is an extending and long-lasting disturbance, nearly ~20% modulation can be seen with the distance ~ 3800 Km to 5000 Km from the cyclone point[42]. In this present work, we found a maximum decrease of foF2 at the time of the maximum cyclone intensity (~0.8 MHz) and land falling day (~2 MHz) during 08-09 UT (15-16 LT). From Fig. 4(b), generally, foF2 shows a maximum during noon due to maximum solar ionization[43]. The local time variation (Fig 4(b) shows the depletion foF2 starts from 05-11 UT (12-18 LT), and the hmF2 shows the increase before 05 UT (12 LT). The observed deep convective activity (~115-120 W/m2) (Fig 5) and upward vertical velocity evidence the deep convection. The weak westward background stratospheric zonal wind will allow the waves to propagate upward (Fig. 6). Recently, Gajalakshmi

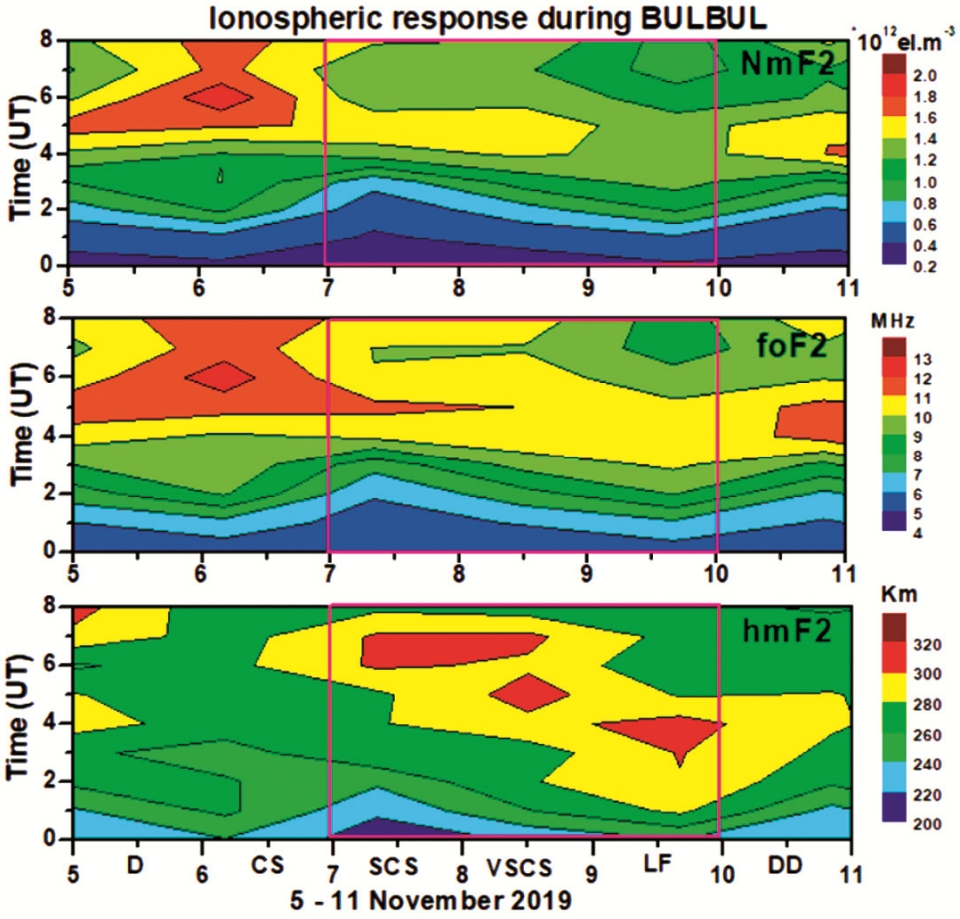

Fig. 7 — Ionospheric foF2, NmF2 and hmF2 variation during cyclone BULBUL.

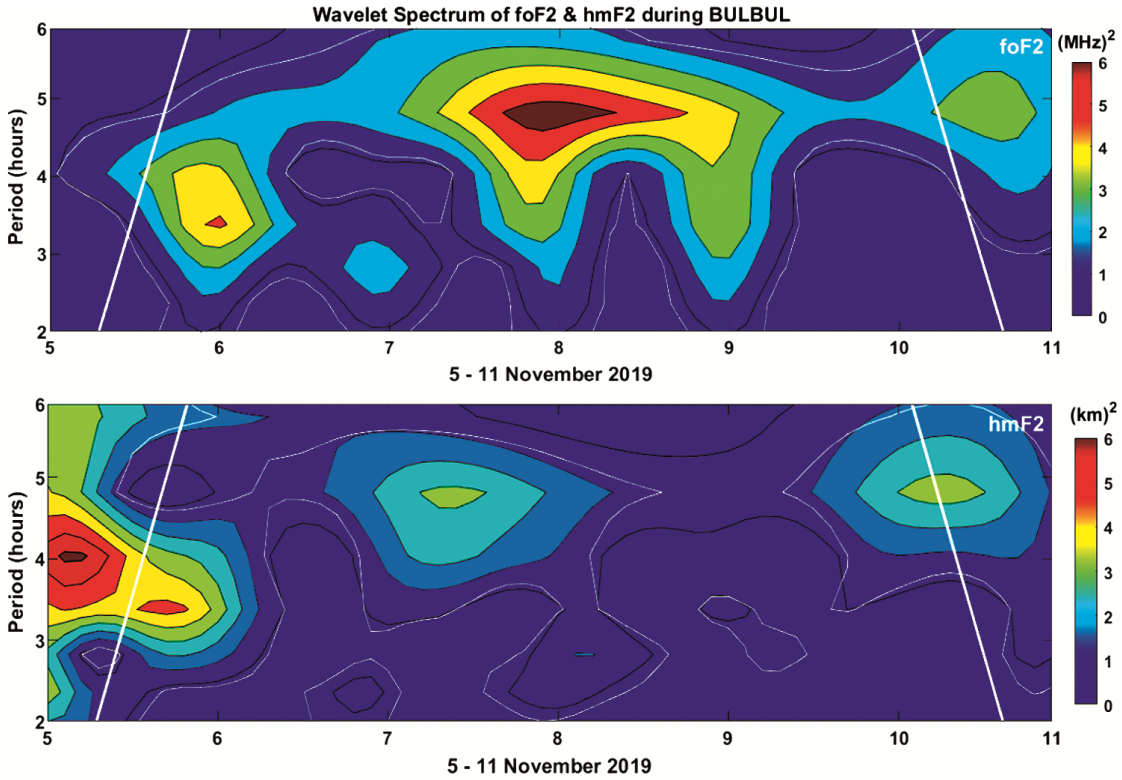

Fig. 8 — Wavelet Power Spectrum of Gravity wave activity during cyclone BULBUL.

et al.,[24] evidenced the gravity wave propagation to ionospheric heights and nearly ~1 MHz foF2 depletion.

4 Conclusion

Tropical ionospheric response to severe cyclonic storm "BULBUL" was investigated using ground ionosonde observations over SANYA (18.34°N, 109.62°E). The foF2 shows significant suppression at the intensified stage and maximum drop during land falling of "BULBUL". A negative correlation between foF2 and cyclone intensity was observed. Hence, the effect of the tropical cyclone is seen as a broadband disturbance and introduces a significant impact on the tropical ionosphere.

Acknowledgement

The author, M.Gajalakshmi, thanks the Director, Centre for Research, Anna University, for the Anna Centenary Research Fellowship grant. The authors thank all the data providing centres/agencies, the WDC for Geophysics, Beijing, Geophysics center, National Earth System Science Data Center ionospheric observation for the ionosonde data, India Meteorological Department (IMD), New Delhi, World Data Centre of Geomagnetism, Kyoto, The Climate Diagnostic Center (CDC) of the National Oceanic and Atmospheric Administration (NOAA) Satellite, The European Centre for Medium-range Weather Forecasts (ECMWF) reanalysis (ERA-5).

References

1 Poulos HM, *Natural Hazards,* 54 (2010)1015.
2 Peduzzi, Pascal, Chatenoux B, Dao H, Bono A D, Herold C, Kossin J, Mouton F & Ola N, *Nature Climate Change*, 4 (2012) 289.
3 Gallina V, Torresan S, Critto A, Sperotto A, Glade T, Gallina M A, Valentina, Torresan S, Critto A, Sperotto A, Glade T & Marcomini A, *J Environ Manag*, 168 (2016) 123.
4 Klotzbach P J, Wood K M, Schreck III C J, Bowen S G, Patricola C M & Bell M M, *GeophysRes Lett*, 6 (2022).
5 Pérez-Alarcón A, Coll-Hidalgo P, Fernández-Alvarez J C, Nieto R & Gimeno L, *Trop Cyclone Res Rev*, 2 (2022) 76.
6 Polyakova A S, Perevalova N P, *Adv Space Res*, 7 (2011) 1196.
7 Polyakova A S, Perevalova N P, *Adv Space Res*, 52 (2013) 1416.
8 Freeshah M, Zhang X, Şentürk E, Adil M A, Mousa B G, Tariq A, Ren X & Refaat M, *Remote Sen*, 4 (2021) 661.
9 Yang Z & Liu Z, *J Geophys Res: Space Phys*, 5 (2016) 4705.
10 Li W, Yue J, Wu S, Yang Y, Li Z, Bi J & Zhang K, *GPS Solutions*, 22 (2018) 1.
11 Guha A, Paul B, Chakraborty M & De B K, *J Geophys Res: Space Phys*, 121 (2016) 5764.
12 Dube A, Singh R, Maurya AK, Kumar S, Sunil P S & Singh A K, *J Geophys Res: Space Phys*, 1 (2020).

13 Chen J, Zhang X, Ren X, Zhang J, Freeshah M & Zhao Z, *Adv Space Res*, 7 (2020) 1743.
14 Song Q, Ding F, Zhang X & Mao T, *J Geophys Res: Space Phys*, 1 (2017) 1055.
15 Fu J & Jin S, *J Geophys Res: Space Phys*, 1 (2023).
16 Rozhnoi A, Solovieva M, Levin B, Hayakawa M & Fedun V, *Natural Hazards Earth Syst Sci*, 10 (2014) 2671.
17 Nina A, Radovanović M, Milovanović B, Kovačević A, Bajčetić J & Popović LČ, *Adv Space Res*, 8 (2017) 1866.
18 Kumar S, NaitAmor S, Chanrion O & Neubert T, *J Geophys Res: Space Phy*, 8 (2017) 8720.
19 NaitAmor S, Cohen M B, Kumar S, Chanrion O & Neubert T, *Geophys Res Lett*, 19 (2018) 10.
20 Das B, Sen A, Pal S & Haldar P K, *J Atmos Sol-Terrestr Phys*, 220 (2021) 105668.
21 Bhagavathiammal G J, Lal M & Emperumal K, *J Atmos Sol-Terrestr Phys*, 211 (2020) 105462.
22 Karthikeyan E, Sathishkumar S, Yasala S, Emperumal K & Ranjit C, *Indian J Sci Technol*, 14 (2021) 2832.
23 Sharan A, *Geomagnetism Aeronomy*, 6 (2022) 802.
24 Gajalakshmi M, Bhagavathiammal G J & Hozumi K, *J Atmos Sol-Terrestr Phys*, 250 (2023) 106120.
25 Zheng Y, Chernogor L F, Garmash K P, Guo Q, Rozumenko V T & Luo Y, *J Geophys Res: Space Phys*, 8 (2022).
26 Vanina-Dart L B, *42nd COSPAR Scientific Assembly*, 42 *(*2018*)* C2-2.
27 Lastovicka J, *J Atmos Sol Terr Phys*, 68(2006) 479.
28 Kníˇzova ´ K P, Moˇsna Z, Kouba D, Potuˇzníkov´ a K & Boˇska, J, *J Atmos Sol Terr Phys*, 136 (2015) 244.
29 Lastovicka J, Sauli P, *Adv Space Res*, 24 (1999) 1473.
30 Afraimovich E L, Kosogorov E A, Leonovich L A, Palamartchouk K S, Perevalova N P & Pirog O M, *J Atmos Sol Terr Phys*, 62 (2000) 553.
31 Lin J W, *J Earth Syst Sci*, 121 (2012) 1001.
32 Ming C F, Z Chen & F Roux, *Ann Geophys*, 28 (2010) 531.
33 Bindu H H, Ratnam M V, Yesubabu V, Rao T N, Eswariah S, Naidu C V & Rao S V, *J Atmos Sol-Terrestr Phys*, 169 (2018) 101.
34 Wang Y, Zhang L, Zhang Y & Guan J, *Geophys Res Lett*, 46 (2019) 4523.
35 Faisal Q A, Hossain M A, Hassan S Q, Rashid T & Meandad J, *Dew-Drop*, 8 (2022) 95.
36 Kumar S, Biswas K & Pandey A K, *Proc AAAI Conf on Artificial Intelligence*, 3517 (2021) 14831.
37 Biswakarma P, Singh M, Sarma A K & Joshi V, *Proc Ind Nat Sci Acad*, 87 (2021) 628.
38 Reinisch B W, Galkin I A, Khmyrov G M, Kozlov A V, Bibl K, Lisysyan I A, Cheney G P, Huang X, Kitrosser D F, Paznukhov V V & Luo Y, *Radio Sci*, 01 (2009) 1.
39 Yu S & Liu Z, *Earth Plant Space*, 73(2021)1.
40 Hersbach H, Bell B, Berrisford P, Hirahara S, Horányi A, Muñoz-Sabater J, Nicolas J, Peubey C, Radu R, Schepers D & Simmons A, *Quarterly J Royal Meteorol Soc*, 730 (2020) 1999.
41 Report from IMD (BULLETIN NO.: 35 (BOB/04/ 2019)).(Ref: https://mausam.imd.gov.in/Forecast/marquee_ data/indian0906.pdf)
42 Vanina-Dart L B, Romanov A A & Sharkov E A, *Geomagnetism Aeronomy*, 51 (2011) 774.
43 Lynn K J, Gardiner-Garden R S & Heitmann A, *J Geophys Res: Space Phys*, 119 (2014) 10.